J|A|C|S
ARTICLES
Published on Web 12/06/2006

Dynamic Processes in [16]Annulene: Möbius Bond-Shifting Routes to Configuration Change

Ryan P. Pemberton, Colleen M. McShane, Claire Castro,* and William L. Karney*

Contribution from the Department of Chemistry, University of San Francisco, 2130 Fulton Street, San Francisco, California 94117-1080

Received August 29, 2006; E-mail: castroc@usfca.edu; karney@usfca.edu

Abstract: Density functional and ab initio methods have been used to study the mechanisms for key dynamic processes of the experimentally known S_4-symmetric [16]annulene (**1a**). Using BH&HLYP/6-311+G** and B3LYP/6-311+G**, we located two viable stepwise pathways with computed energy barriers ($E_a = 8-10$ kcal/mol) for conformational automerization of **1a**, in agreement with experimental data. The transition states connecting these conformational minima have Möbius topology and serve as starting points for nondegenerate π-bond shifting (configuration change) via Möbius aromatic transition states. The key transition state, **TS1**−**2**, that connects the two isomers of [16]annulene (CTCTCTCT, **1** → CTCTTCTT, **2**) has an energy, relative to the S_4 isomer, that ranged from 6.9 kcal/mol (B3LYP/6-311+G**) to 16.7 kcal/mol (BH&HLYP/6-311+G**), bracketing the experimental barrier. At our best level of theory, CCSD(T)/cc-pVDZ-(est), this barrier is 13.7 kcal/mol. Several other Möbius bond-shifting transition states, as well as Möbius topology conformational minima, were found with BH&HLYP energies within 22 kcal/mol of **1a**, indicating that many possibilities exist for facile thermal configuration change in [16]annulene. This bond-shifting mechanism and the corresponding low barriers contrast sharply with those observed for cis/trans isomerization in acyclic polyenes, which occurs via singlet diradical transition states. All Möbius bond-shifting transition states located in [16]- and [12]annulene were found to have RHF → UHF instabilities with the BH&HLYP method but not with B3LYP. This result appears to be an artifact of the BH&HLYP method. These findings support the idea that facile thermal configuration change in [4*n*]annulenes can be accounted for by mechanisms involving twist-coupled bond shifting.

Introduction

The 1960s through the early 1970s was an active period for the synthesis and study of the dynamic processes of medium- and large-sized annulenes.[1] The work from this time was aptly summarized in a seminal paper by Oth, which fully describes the various syntheses and outlines possible dynamic processes (often with experimental barriers determined from variable temperature NMR studies) for [8]-, [12]-, [14]-, [16]-, and [18]-annulene.[2] From that paper, several conclusions emerged: (1) floppier annulenes undergo facile thermal cis/trans isomerization, making it difficult to have only one configuration in solution; (2) bond shifting passes through a (nearly) planar transition state; (3) the barrier to ring closure reactions is often higher than the barriers for configuration and conformation change.

A resurgence of interest in annulenes has occurred in more recent years,[3] motivated in part by the ability to run sophisticated calculations[4] and in part by a renewed desire to probe aromaticity.[5] Within the [4*n*]annulenes, research has focused on both the antiaromaticity of planar species[6] and the potential aromaticity of species with Möbius topology.[7−10] Recently, we reported a possible explanation for the known[11] facile cis/trans isomerization in [12]annulene, using DFT and coupled cluster computations.[12] We postulated that this configuration change results from π-bond shifting, via a nonplanar Möbius aromatic transition state—a mechanism we called "twist-coupled bond shifting". Questions remain, such as: Is Möbius bond shifting

(1) Reviews: (a) Sondheimer, F. The Annulenes. *Acc. Chem. Res.* **1972**, *5*, 81. (b) Balaban, A. T.; Banciu, M.; Ciorba, V. *Annulenes, Benzo-, Hetero-, Homo-Derivatives, and their Valence Isomers*, Vol. I; CRC Press: Boca Raton, FL, 1987; Chapter 4.
(2) Oth, J. F. M. *Pure Appl. Chem.* **1971**, *25*, 573.
(3) (a) Kennedy, R. D.; Lloyd, D.; McNab, H. *J. Chem. Soc. Perkin Trans. 1* **2002**, 1601. (b) Spitler, E. L.; Johnson, C. A.; Haley, M. M. *Chem. Rev.* **2006**, doi: 10.102/cr050541c (published on web 9/19/2006).
(4) See, for example, the case of [10]annulene: (a) Sulzbach, H. M.; Schaefer, H. F.; Klopper, W.; Lüthi, H. P. *J. Am. Chem. Soc.* **1996**, *118*, 3519. (b) King, R. A.; Crawford, T. D.; Stanton, J. F.; Schaefer, H. F. *J. Am. Chem. Soc.* **1999**, *121*, 10788. (c) Price, D. R.; Stanton, J. F. *Org. Lett.* **2002**, *4*, 2809. (d) Castro, C.; Karney, W. L.; McShane, C. M.; Pemberton, R. P. *J. Org. Chem.* **2006**, *71*, 3001.
(5) For recent reviews of aromaticity, see: (a) Schleyer, P. v. R., Ed. *Chem. Rev.* **2001**, *101* (May). (b) Schleyer, P. v. R., Ed. *Chem. Rev.* **2005**, *105*, (October).
(6) Wiberg, K. B. *Chem. Rev.* **2001**, *101*, 1317.
(7) Heilbronner, E. *Tetrahedron Lett.* **1964**, 1923.
(8) (a) Mauksch, M.; Gogonea, V.; Jiao, H.; Schleyer, P. v. R. *Angew. Chem. Int. Ed. Engl.* **1998**, *37*, 2395. (b) Martín-Santamaría, S.; Lavan, B.; Rzepa, H. S. *J. Chem. Soc. Perkin Trans. 2* **2000**, 1415. (c) Havenith, R. W. A.; van Lenthe, J. H.; Jenneskens, L. W. *Int. J. Quantum Chem.* **2001**, *85*, 52. (d) Castro, C.; Isborn, C. M.; Karney, W. L.; Mauksch, M.; Schleyer, P. v. R. *Org. Lett.* **2002**, *4*, 3431.
(9) For the synthesis of a substituted [16]annulene with Möbius topology and an investigation of its aromaticity, see: (a) Ajami, D.; Oeckler, O.; Simon, A.; Herges, R. *Nature* **2003**, *426*, 819. (b) Castro, C.; Chen, Z.; Wannere, C. S.; Jiao, H.; Karney, W. L.; Mauksch, M.; Puchta, R.; Hommes, N. J. R. v. E.; Schleyer, P. v. R. *J. Am. Chem. Soc.* **2005**, *127*, 2425. (c) Ajami, D.; Hess, K.; Köhler, F.; Näther, C.; Oeckler, O.; Simon, A.; Yamamoto, C.; Okamoto, Y.; Herges, R. *Chem. Eur. J.* **2006**, *12*, 5434.
(10) Review: Rzepa, H. S. *Chem. Rev.* **2005**, *105*, 3697.

10.1021/ja066152x CCC: $33.50

Scheme 1

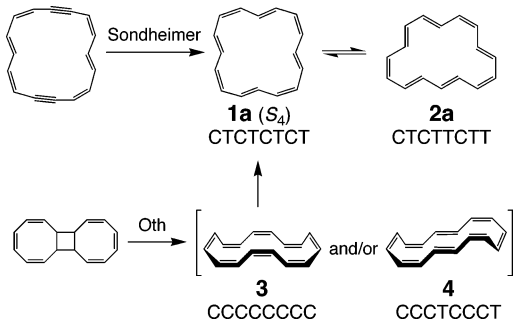

generally facile in [16]annulene? Are there Möbius conformational minima in solution? Here we describe our computational results on the dynamic processes of [16]annulene, with particular attention given to both twist-coupled bond shifting and conformational change. Finally, we highlight the pitfalls in using certain density functional methods when studying the annulenes.

Background

[16]Annulene was synthesized initially by Sondheimer[13] and later by Oth and Schröder.[14,15] Regardless of the path for formation, the [16]annulene species observed by solution NMR appeared to be a mixture of configurational isomers **1a (**major) and **2a** (minor) at temperatures as low as −67 °C (Scheme 1).[2,16] X-ray analysis of the major product revealed it to have a nearly S_4 symmetric bond-alternating structure.[17]

In Oth and Schröder's synthesis of [16]annulene, the presumed product of photochemical ring opening of COT dimer (**3** and/or **4**) was never detected, suggesting that the initial photoproduct undergoes rapid configuration change to yield the major observed isomer **1a**.[2] In solution, **1a** is in equilibrium with the minor isomer **2a**, even at −130 °C. Using variable-temperature NMR, Oth determined a barrier of 10.3 kcal/mol for this process.[2] This remarkably low barrier is much lower than that for thermal cis/trans isomerization in acyclic polyenes of similar conjugation length.[18] At −30 °C, the NMR spectrum of [16]annulene appears as one peak (6.74 ppm δ), indicating magnetic equivalence of all 16 protons, resulting from a combination of the dynamic processes shown in Scheme 2.

According to the results and interpretations of Oth, [16]-annulene differs from [12]annulene in two key respects: (1) [16]annulene *does* undergo planar degenerate bond shifting (**1a** → **1a′′**) and with a lower barrier than for conformational automerization and (2) [16]annulene undergoes configurational isomerization (**1a** → **2a**) more easily ($E_a \sim 10$ kcal/mol) than it undergoes electrocyclization ($E_a \sim 22$ kcal/mol)[19] (Scheme 3).

Scheme 2 [a]

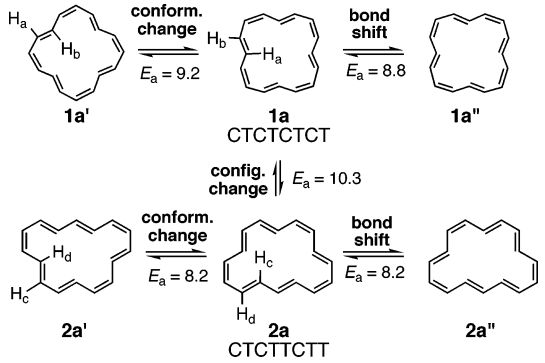

[a] Energies in kcal/mol.

Scheme 3

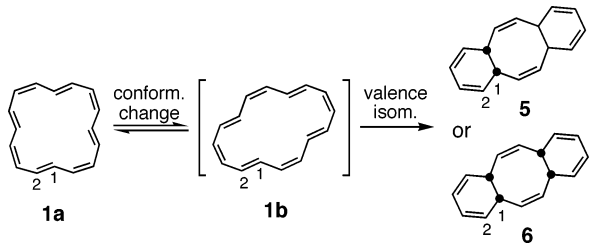

Several research groups have used computations to probe the potential energy surface of [16]annulene.[8b,8d,9c,20] While most of these calculations focused on highlighting conformational minima, Lee and Li did present ab initio and DFT results for barriers associated with electrocyclization of conformer **1b** → **5/6**.[20b] This study also supported earlier conclusions by Rzepa[10] that **6** is thermodynamically more stable than **5** and is thus the likely product of electrocyclization rather than **5**, the isomer put forth by Oth.[19] There are no reported studies of the conformational conversion of **1a** to **1b** nor, in fact, of any of the processes outlined in Scheme 2.

As part of our ongoing investigation of the scope of Möbius bond shifting as a mechanism for configuration change in annulenes, we describe here our findings for the interconversion of **1** and **2**. In addition, we present results on the conformational mobility of both **1** and **2**. The combination of these configurational and conformational results can explain the experimental observations for [16]annulene. Finally, we address the use of representative DFT methods for highly nonplanar bond-shifting transition states.

Computational Methods

Geometries of stationary points were optimized using the B3LYP[21] and BH&HLYP[22] density functional methods, coupled with the 6-311+G(d,p) triple-ζ basis set[23] (henceforth denoted as "TZ"), which includes one set of d functions on each carbon, one set of p functions on each hydrogen, and one set of diffuse functions on each carbon. BH&HLYP is known to yield better annulene geometries for evaluating magnetic properties as well as better relative energies, compared to

(11) (a) Oth, J. F. M.; Röttele, H.; Schröder, G. *Tetrahedron Lett.* **1970**, 61. (b) Oth, J. F. M.; Gilles, J.-M.; Schröder, G. *Tetrahedron Lett.* **1970**, 67.
(12) Castro, C.; Karney, W. L.; Valencia, M. A.; Vu, C. M. H.; Pemberton, R. P. *J. Am. Chem. Soc.* **2005**, *127*, 9704.
(13) (a) Sondheimer, F.; Gaoni, Y. *J. Am. Chem. Soc.* **1961**, *83*, 4863. (b) Calder, I. C.; Gaoni, Y.; Sondheimer, F. *J. Am. Chem. Soc.* **1968**, *90*, 4946.
(14) Schröder, G.; Oth, J. F. *Tetrahedron Lett.* **1966**, 4083.
(15) For syntheses of [16]annulene that involve deuteration, see: (a) Stevenson, C. D.; Kurth, T. L. *J. Am. Chem. Soc.* **1999**, *121*, 1623. (b) Stevenson, C. D.; Kurth, T. L. *J. Am. Chem. Soc* **2000**, *122*, 722.
(16) Oth, J. F. M.; Gilles, J.-M. *Tetrahedron Lett.* **1968**, 6259.
(17) (a) Johnson, S. M.; Paul, I. C. *J. Am. Chem. Soc.* **1968**, *90*, 643. (b) Johnson, S. M.; Paul, I. C.; King, G. S. D. *J. Chem. Soc. (B)* **1970**, 643.
(18) For example, an acyclic heptaene was found to have an isomerization barrier of 28 kcal/mol: Doering, W. v. E.; Kitagawa, T. *J. Am. Chem. Soc.* **1991**, *113*, 4288.
(19) Schröder, G.; Martin, W.; Oth, J. F. M. *Angew. Chem. Int. Ed. Engl.* **1967**, *6*, 870.
(20) (a) Hernando, J. M.; Quirante, J. J.; Enríquez, F. *Collect. Czech. Chem. Commun.* **1992**, *57*, 1. (b) Lee, H.-L.; Li, W.-L. *Org. Biomol. Chem.* **2003**, *1*, 2748.
(21) (a) Becke, A. D. *J. Chem. Phys.* **1993**, *98*, 5648. (b) Lee, C.; Yang, W.; Parr, R. G. *Phys. Rev. B* **1988**, *37*, 785.
(22) (a) Becke, A. D. *J. Chem. Phys.* **1992**, *98*, 1372. (b) Miehlich, B.; Savin, A.; Stoll, H.; Preuss, H. *Chem. Phys. Lett.* **1989**, *157*, 200.
(23) Hariharan, P. C.; Pople, J. A. *Theor. Chim. Acta* **1973**, *28*, 213.

B3LYP.[24,25] The B3LYP geometries were obtained for comparison purposes and for bracketing of bond-shifting barriers (vide infra). Vibrational frequency analyses were performed at the same levels as the optimizations to verify that stationary points were either minima or transition states and to obtain zero-point energies (ZPEs) for correction of relative energies. All bond-shifting transition states were subjected to intrinsic reaction coordinate (IRC) calculations to determine the structures of the nearest minima.

In order to obtain more reliable relative energies, single-point energies were computed using coupled-cluster theory with single and double substitutions and a perturbative correction for triple excitations [CCSD(T)].[26] CCSD(T) calculations employed the 6-31G* basis set.[23] The BH&HLYP/TZ optimized geometries were used for these single-point energies because this optimization method was found[24] to give the best results for the relative energies of the [10]annulene isomers, in good agreement with more expensive CCSD(T) calculations.

The determination of reliable CCSD(T) relative energies for bond-alternating versus bond-equalized annulenes requires the use of at least a double-ζ basis set with polarization functions on both carbon and hydrogen,[4b] such as Dunning's correlation-consistent polarized valence double-ζ basis set (cc-pVDZ).[27] Because CCSD(T)/cc-pVDZ calculations on these systems were beyond our capabilities, we estimated the effect of increasing the basis set from 6-31G* to cc-pVDZ by computing MP2/cc-pVDZ energies and then scaling the CCSD(T) correlation energy according to the method of Bally and McMahon.[28] The energy is estimated using the equation

$$E[\text{CCSD(T)/cc-pVDZ(est)}] = E(\text{HF/cc-pVDZ}) + \frac{E_{\text{corr}}(\text{MP2/cc-pVDZ})}{E_{\text{corr}}(\text{MP2/6-31G*})} E_{\text{corr}}[\text{CCSD(T)/6-31G*}]$$

where E(HF/cc-pVDZ) is the Hartree−Fock energy and E_{corr} is the correlation energy at the designated level of theory. Unless otherwise specified, energies referred to in the text pertain to the CCSD(T)/cc-pVDZ(est)//BH&HLYP/TZ + ZPE level of theory.

To assess aromatic character, nucleus independent chemical shifts (NICS)[29] for selected species were computed using the GIAO method at the B3LYP/TZ level on the BH&HLYP/TZ geometries. Bond-shifting transition states were tested for RHF → UHF instabilities, and species with such instabilities were re-optimized with an unrestricted wave function. All calculations were performed using Gaussian 98 and Gaussian 03.[30] Structures were visualized with MacMolPlt,[31] and orbitals were visualized with Molden.[32]

Results and Discussion

For reference purposes, Figure 1 shows the BH&HLYP/TZ optimized geometries of **1a** and **2a**, the two configurational isomers that are in equilibrium in solution. Both are strongly bond alternating and differ in energy by ca. 2 kcal/mol using DFT methods but less than 1 kcal/mol using CCSD(T)/cc-pVDZ(est) (Table 1). This small energy difference is consistent with the observation of an 83:17 equilibrium mixture of **1a** and **2a** in solution at −140 °C.[33]

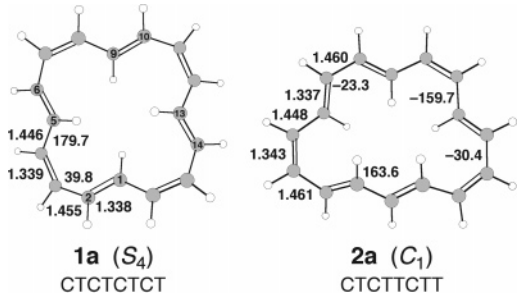

Figure 1. BH&HLYP/TZ optimized structures of CTCTCTCT (**1a**, major isomer) and CTCTTCTT (**2a**, minor isomer) [16]annulene. Selected C−C bond lengths (Å) and CCCC dihedral angles (°) are shown.

Conformation Change. Relative energies of conformational minima and corresponding transition states are given in Table 1. We were primarily interested in two conformational processes: (i) conformational automerization in **1** (**1a** → **1a′**, Scheme 2) and (ii) conversion of **1a** to **1b**, the conformation that can undergo thermal electrocyclic ring closure (Scheme 3).

For both processes, we considered the possibility of concerted conformation change (analogous to our earlier findings for [12]-annulene[25]), but no transition states could be located for such pathways. In both cases, stepwise mechanisms emerged. The two stepwise paths with the lowest overall barriers connecting **1a** and **1a′** are depicted in Figure 2.[35] The main difference between the two paths is whether, after rotating the first trans C═C bond ("T1"), an adjacent (T2) or opposite (T3) trans C═C bond is rotated next. If two opposite trans C═C bonds are rotated in sequence, the mechanism proceeds via **1b** (top path), the conformation that presumably undergoes ring closure at 30 °C.[19] If the T2 trans C═C bond is rotated after T1, the mechanism proceeds via **1d** (bottom path). The structures of the intermediates and transition states for these two paths are shown in Figure 3. Figure 4 summarizes the BH&HLYP/TZ energetics for the two pathways. The results indicate that passage through intermediate **1d** (bottom path) is favored over passage via **1b** by 1.5 kcal/mol (Figure 4, Table 1).

The ca. 8 kcal/mol computed barrier for the mechanism via **1d** is below Oth's experimental barrier of 9.2 kcal/mol.[2] The barrier for the alternate process via **1b** is slightly higher than the experimental barrier, indicating that this is also a competitive path for conformation change. All methods, including CCSD(T)/cc-pVDZ(est), predict the path via **1d** to have a lower activation energy than that via **1b**. However, at the CCSD(T) level **1d** is no longer a discrete intermediate; rather, **1d** and **TS1c1d** are isoenergetic points on a plateau, separating equivalent **1c** conformers (Table 1). Thus *two* mechanisms are possible to effect conformational automerization: at lower temperatures path T1−T2−T3−T4 occurs; at higher temperature T1−T3−T2−T4 becomes possible and also provides the requisite conformation for ring closure.

The results indicate that, among the [4*n*]annulenes, [16]-annulene is the first example in which clear multistep mecha-

(24) Wannere, C. S.; Sattelmeyer, K. W.; Schaefer, H. F.; Schleyer, P. v. R. *Angew. Chem. Int. Ed.* **2004**, *43*, 4200.
(25) Castro, C.; Karney, W. L.; Vu, C. M. H.; Burkhardt, S. E.; Valencia, M. A. *J. Org. Chem.* **2005**, *70*, 3602.
(26) (a) Bartlett, R. J. *J. Phys. Chem.* **1989**, *93*, 1697. (b) Raghavachari, K.; Trucks, G. W.; Pople, J. A.; Head-Gordon, M. *Chem. Phys. Lett.* **1989**, *157*, 479. (c) Scuseria, G. E. *Chem. Phys. Lett.* **1991**, *176*, 27.
(27) Dunning, T. H., Jr. *J. Chem. Phys.* **1989**, *90*, 1007.
(28) (a) Matzinger, S.; Bally, T.; Patterson, E. V.; McMahon, R. J. *J. Am. Chem. Soc.* **1996**, *118*, 1535. (b) This is similar to the "scaling all correlation" (SAC) method of Truhlar: Rossi, I.; Truhlar, D. G. *Chem. Phys. Lett.* **1995**, *234*, 64.
(29) Schleyer, P. v. R.; Maerker, C.; Dransfeld, A.; Jiao, H.; Hommes, N. J. R. v. E. *J. Am. Chem. Soc.* **1996**, *118*, 6317.
(30) (a) Frisch, M. J.; et al. *Gaussian 98*, Revision A.11.3; Gaussian, Inc.: Pittsburgh, PA, 2002. (b) Frisch, M. J.; et al. *Gaussian 03*, Revision D.01; Gaussian, Inc., Wallingford, CT, 2004.
(31) MacMolPlt v.5.3.5: Bode, B. M.; Gordon, M. S. *J. Mol. Graphics Modell.* **1998**, *16*, 133.
(32) Schaftenaar, G.; Noordik, J. H. *J. Comput.-Aided Mol. Des.* **2000**, *14*, 123.
(33) Oth, J. F. M.; Anthoine, G.; Gilles, J.-M. *Tetrahedron Lett.* **1968**, 6265.
(34) Conformer **1b** was also studied with C_2, C_s, and C_1 symmetry. Despite the C_2 and C_1 symmetric forms having no imaginary frequencies, the C_{2v} form was lowest in energy after ZPE correction.
(35) Other paths are possible, but these have higher barriers than the paths in Figure 2.

Table 1. Relative Energies (kcal/mol) and Aromaticity Indicators of [16]Annulene Stationary Points[a]

			BH&HLYP/6-311+G**				B3LYP/6-311+G**			CCSD(T)/ 6-31G*[c]	CCSD(T)/cc-pVDZ(est)[c]
species	sym	config	rel E	NI	Δr[d]	NICS(0)[e]	rel E	NI	Δr[d]	rel E	rel E
1a	S_4	CTCTCTCT	0.0	0	0.118	+6.4	0.0	0	0.100	0.0	0.0
TS1a1c	C_1	CTCTCTCT	8.1	1	0.149	−0.9	8.2	1	0.138	7.3	7.9
1c	C_1	CTCTCTCT	5.3	0	0.126	+4.6	5.0	0	0.107	5.9	5.4
TS1c1b	C_1	CTCTCTCT	9.7	1	0.146	−0.8	9.4	1	0.134	9.3	9.4
1b	C_{2v}	CTCTCTCT	5.3	1[b]	0.122	+3.7	6.6	1[b]	0.104	6.6	5.6
TS1c1d	C_1	CTCTCTCT	8.2	1	0.149	−1.0	8.0	1	0.141	7.6	7.7
1d	C_s	CTCTCTCT	7.6	0	0.129	+3.2	7.8	0	0.109	8.1	7.7
TS1a1e	C_1	CTCTCTCT	7.6	1	0.145	+1.3	7.1	1	0.136	7.3	7.1
1e	C_1	CTCTCTCT	6.1	0	0.125	−2.3	4.9	0	0.102	5.0	5.1
TS1−2	C_1		16.7	1	0.019	−14.2	6.9	1	0.025	16.1	13.7
2b	C_1	CTCTTCTT	5.3	0	0.125	+5.9	4.7	0	0.110	4.7	4.1
TS2a2b	C_1	CTCTTCTT	8.4	1	0.158	+0.6	8.6	1	0.150	6.4	6.7
2a	C_1	CTCTTCTT	2.3	0	0.124	+7.3	2.1	0	0.109	1.2	0.8

[a] NI = number of imaginary frequencies. [b] See ref 33. [c] Computed at the BH&HLYP/6-311+G** geometry. [d] Δr = difference, in Å, between the longest and shortest C−C bonds. [e] Computed using the GIAO-B3LYP/6-311+G** method at the BH&HLYP/6-311+G** geometry.

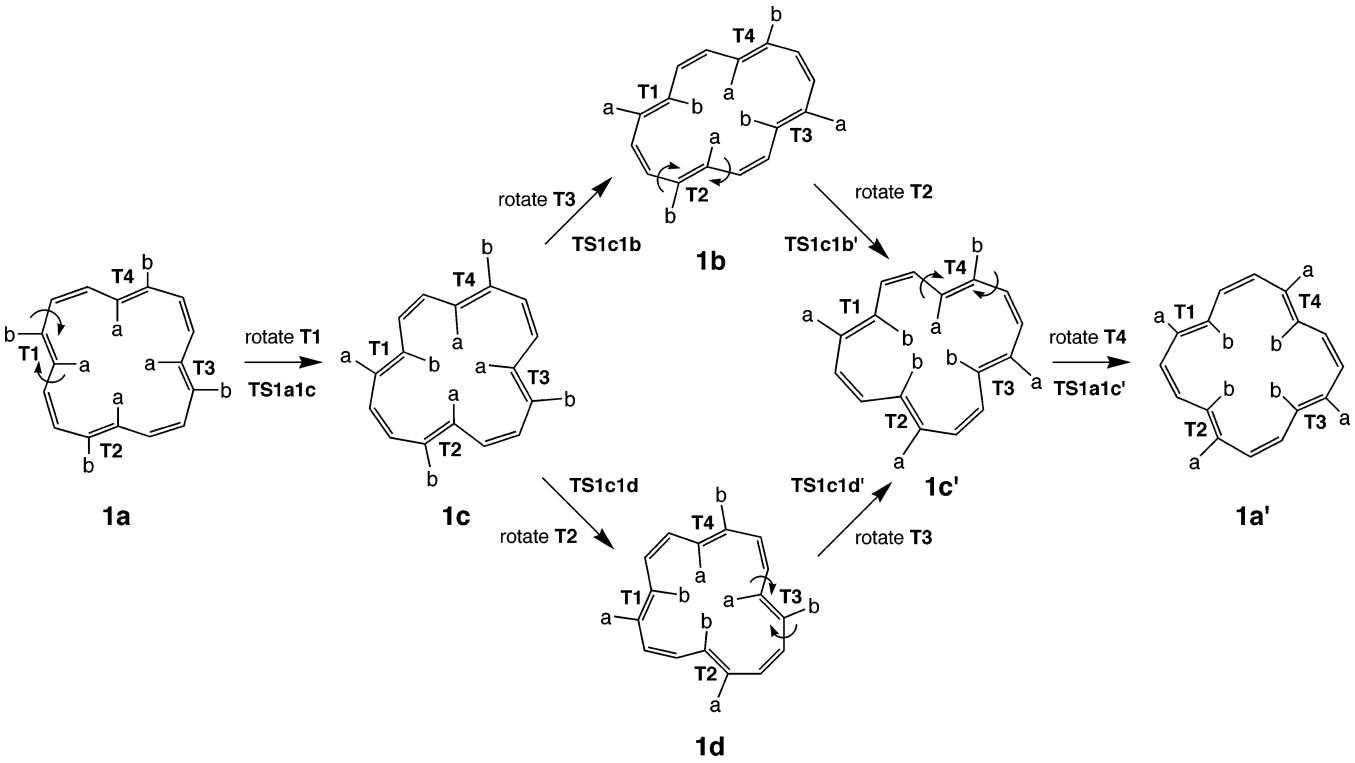

Figure 2. Two possible pathways for degenerate conformation change in CTCTCTCT [16]annulene (**1a**). Trans C═C bonds are labeled T1, T2, etc. Labels near the arrows indicate the relevant transition state as well as which trans C═C bond is rotating.

nisms exist for degenerate conformation change. Both the processes presented here involve at least two intermediate conformations upon stepwise rotation of the trans C═C bonds. This is in stark contrast with the concerted but asynchronous mechanism found for [12]annulene[25] and with concerted ring inversion in cyclooctatetraene.[36]

The conformational transition states (**TS1a1c**, **TS1c1b**, and **TS1c1d** shown in Figure 3) have nominal Möbius topology,[37] yet none are aromatic based on small NICS values and large Δr values (difference between the longest and shortest bond lengths, Table 1). In fact, for these transition states the Δr values are very similar (as are the energies) regardless of whether BH&HLYP or B3LYP is used. Thus, although B3LYP has been criticized for overestimating delocalization in annulenes[24] and other systems,[38] this is obviously only an issue if the molecule has a geometry that allows good π overlap. Clearly, in these cases the large torsional angles (e.g., 71° in **TS1a1c**) preclude effective overlap. Nevertheless, that automerization proceeds via this type of topology becomes important when trying to locate potential starting points for Möbius bond shifting.

In addition to the species involved in the pathways just described, we also located a conformational *minimum* of CTCTCTCT [16]annulene with clear Möbius topology (**1e**, Figure 3).[39] The worst torsional angle in **1e** is 59°. This species

(36) (a) Anet, F. A. L.; Bourn, A. J. R.; Lin, Y. S. *J. Am. Chem. Soc.* **1964**, *86*, 3576. (b) Hrovat, D. A.; Borden, W. T. *J. Am. Chem. Soc.* **1992**, *114*, 5879. (c) Paquette, L. A. *Acc. Chem. Res.* **1993**, *26*, 57. (d) Wenthold, P. G.; Hrovat, D. A.; Borden, W. T.; Lineberger, W. C. *Science* **1996**, *272*, 1456.

(37) An annulene with "Möbius topology" has an odd number of CCCC dihedral angles (ω) with $180° \geq |\omega| > 90°$. Annulenes with "Hückel topology" have an even number of such dihedral angles.

(38) Cramer, C. J. *Essentials of Computational Chemistry*: *Theories and Models*, 2nd ed.; Wiley: New York, 2004; pp. 279−280 and references cited therein.

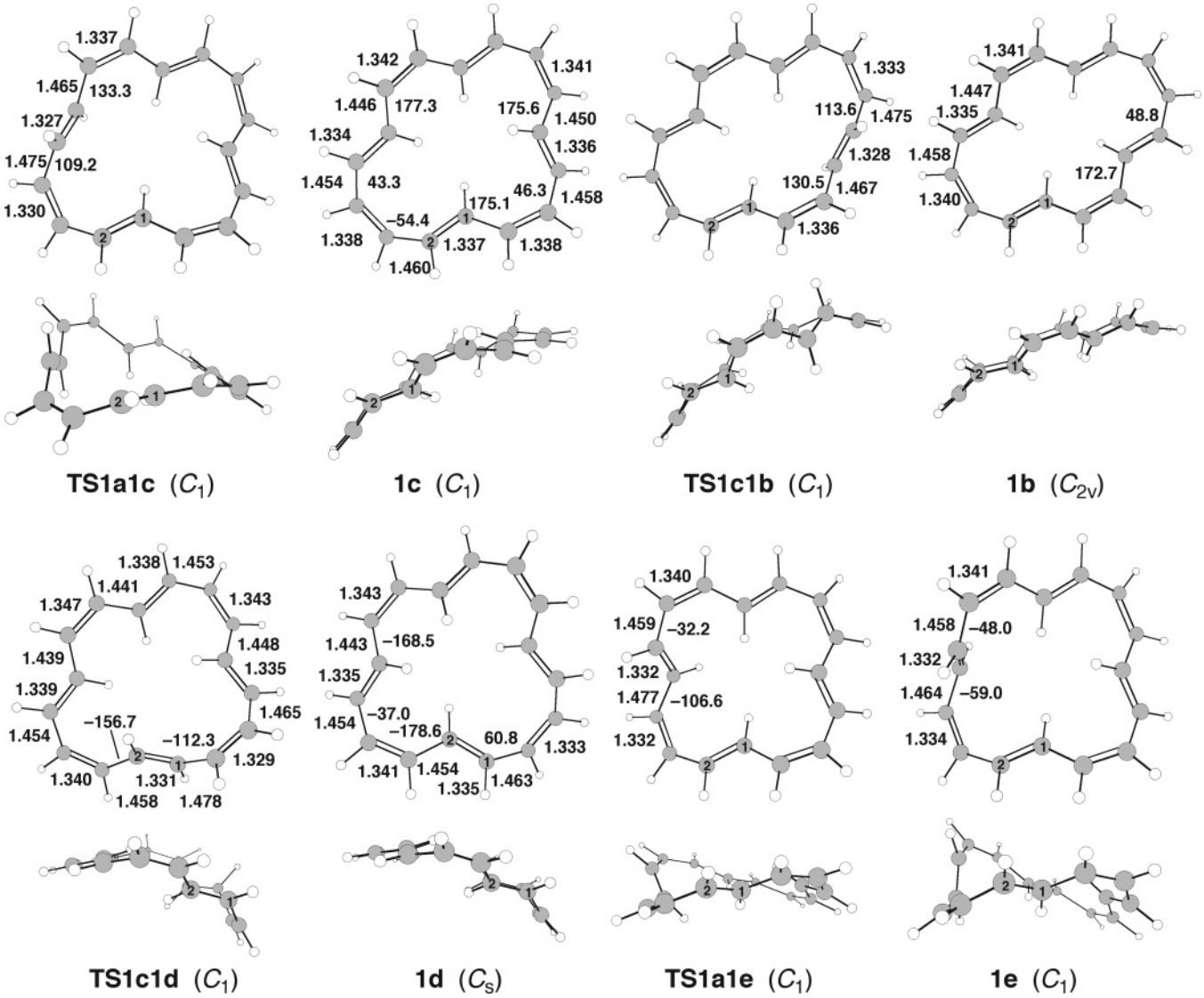

Figure 3. BH&HLYP/TZ optimized structures of stationary points related to conformation change in CTCTCTCT [16]annulene (**1**). Side views of each species are also provided. Selected C−C distances (Å) and CCCC dihedral angles (°) are shown.

is obtained from **1a** simply by rotating T1 (Figure 2) in the opposite direction from that required for forming **1c**. The relative energy (5.1 kcal/mol compared to **1a**) and the barrier to rotation (7.1 kcal/mol from **1a**) suggest that **1e** is readily accessible from **1a** at temperatures at which automerization occurs. Relative to the conformational transition states, **1e** is significantly more delocalized, based on Δr values and on the fact that it is the only bond-alternating structure for which the relative energy decreases by more than 1 kcal/mol upon going from BH&HLYP to B3LYP. The small NICS value (−2.3 ppm) indicates the origin of this delocalization does not arise from aromaticity but rather arises from enhanced conjugation of a polyene.[40] Finally, **1e** is the only minimum that is connected on the PES via a Hückel topology (rather than a Möbius topology) transition state. While **1e** is nonaromatic,[40] its Möbius topology suggests that twist-coupled bond shifting from this minimum should be facile (vide infra).

Configuration Change: 1 → 2. The configuration change of primary interest is the interconversion of **1** and **2** (Scheme 1). Oth proposed a mechanism for this process: "... the passage from [**1** to **2**] would be a sequence of non-isodynamical conformational changes and non-isodynamical bond shifts ... A direct transformation [from **1** to **2**] implying only one bond shift, is difficult to envisage unless the bond shift is taking place in a highly distorted and strained conformation."[2] We hoped to show that such a transformation would in fact not be difficult.

Inspection of models suggested to us that the configuration change of **1** to **2** might occur in one step, involving twist-coupled bond shifting via a Möbius aromatic transition state. In particular, **TS1c1d** from the conformational automerization mechanism (Figure 3) appeared to be a good starting point for Möbius bond shifting to give the desired configuration change. The s-cis and s-trans C−C bonds would become cis and trans C=C bonds, respectively, in the bond-shifting product. If such a pathway occurred it would be analogous to the case of cyclooctatetraene (COT), for which the transition state for ring inversion is the starting point for bond shifting.[36] Unlike the

(39) Several conformations of **1**, including two Möbius ones, were reported (B3LYP) in ref 9c, although no structures were provided. It is possible that one of these is similar to **1e**.

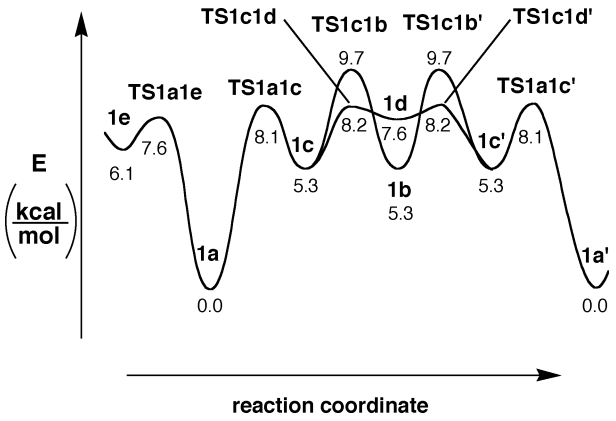

Figure 4. Energy diagram (BH&HLYP/TZ) for two pathways for degenerate conformation change in **1a**. The connection between **1a** and Möbius conformer **1e** is also shown.

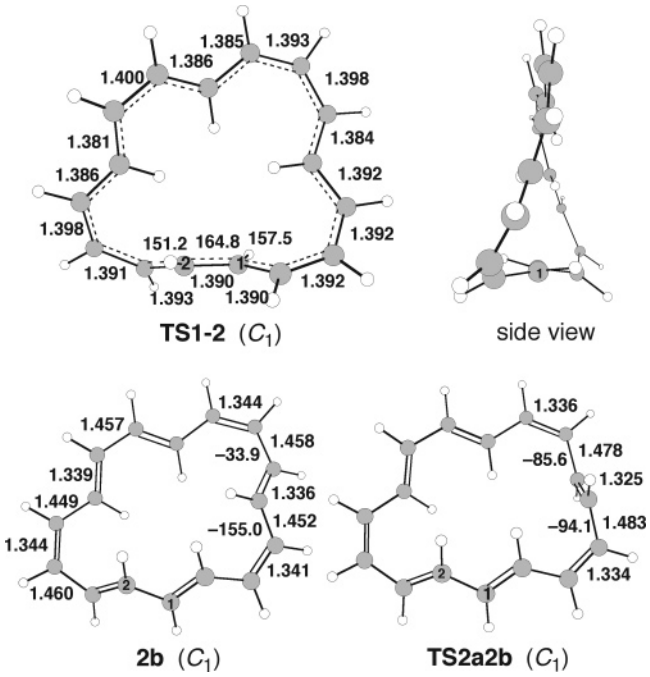

Figure 5. BH&HLYP/TZ optimized structures of the Möbius bond-shifting transition state (**TS1**−**2**) connecting CTCTCTCT (**1**) and CTCTTCTT (**2**) [16]annulene, plus stationary points between this transition state and **2a**. Selected C−C distances (Å) and CCCC dihedral angles (°) are shown.

case of COT, which undergoes degenerate bond shifting, Möbius bond shifting in [16]annulene would be non-degenerate.

Our computational results (Table 1) do indeed show that a viable transition state (**TS1**−**2**, Figure 5) for configuration change can arise from the transition state **TS1c1d** for conformational change. Figure 5 depicts the structure of this very aromatic Möbius, bond-shifting transition state (NICS = −14.2 ppm, Δr = 0.019 Å, worst CCCC torsional angle, 29°). IRC calculations reveal that **TS1**−**2** leads to the desired CTCTTCTT configuration in conformer **2b**, which then can convert to **2a** via a small (3.1 kcal/mol) barrier.

The overall process from **1a** to **2a** consists of (1) conformation change from **1a** to **1c**, and then approximately to a conformational transition state (**TS1c1d)** that is also a starting point for

(40) At the BH&HLYP/TZ level, planar all-*trans* C_{2h} hexadeca-1,3,5,7,9,11,-13,15-octaene has Δr = 0.116 Å. Species **1e** has Δr = 0.125 Å (i.e., it is less delocalized than an acyclic polyene of similar conjugation length). So it is difficult to argue that **1e** is aromatic.

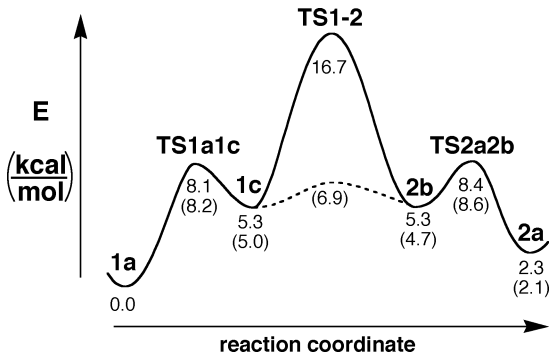

Figure 6. Energy diagram for configuration change (cis/trans isomerization) of **1a** to **2a**. BH&HLYP/TZ relative energies are shown, with B3LYP/TZ values in parentheses.

Table 2. Comparison of Barriers (kcal/mol) for Twist-Coupled Bond Shifting in Annulenes

system	BH&HLYP/TZ[a]	B3LYP/TZ[a]	CCSD(T)/cc-pVDZ[b]	expt
	[10]Annulene			
CCCCT → CCCCT[c]	19.0[c]	11.4	16.1[c]	
	[12]Annulenes			
CTCTCT → CCCTCT[d]	20.2[d]	12.1	18.0[d]	17.4[e]
CTCTCT → CCTCCT[d]	27.8[d]	19.0	25.5[d]	

[a] Corrected for unscaled zero-point energy at the same level. [b] Computed at the BH&HLYP/TZ geometry and corrected for unscaled BH&HLYP/TZ zero-point energy. [c] Degenerate two-twist bond shifting. See ref 4d.[d] Ref 12. [e] Ref 11a.

Möbius bond shifting; (2) twist-coupled bond shifting via a Möbius aromatic transition state (**TS1**−**2**), leading to **2b**; and (3) conformational conversion of **2b** to **2a**. Figure 6 summarizes the energetics of the process.

The energy difference between the S_4 minimum (**1a**) and the crucial transition state (**TS1**−**2**) that connects the two isomers depends on the DFT method, ranging from 16.7 kcal/mol (BH&HLYP/TZ) to 6.9 kcal/mol (B3LYP/TZ) (Table 1). Considering that B3LYP overestimates delocalization,[24,38] the B3LYP barrier is almost certainly too low. At the same time, BH&HLYP generally overestimates barriers for twist-coupled bond shifting.[4d,12] Thus, it would be expected that the true barrier would be found somewhere between 7 and 17 kcal, which is indeed the case (experimental = 10.3 kcal/mol). For such processes in [10]- and [12]annulene, the BH&HLYP barriers are ca. 8−9 kcal/mol higher than the B3LYP barriers, and CCSD(T)/cc-pVDZ barriers lie in between the two (Table 2).

Finally, for this mechanism to explain the experimental result of facile thermal cis/trans isomerization, the computed barrier for configuration change *must be lower* than the experimental barrier for ring closure (22 kcal/mol) *yet higher* than the barrier for conformational automerization (ca. 9 kcal/mol).[2] This is indeed the case for the BH&HLYP/TZ energies but is not the case using the B3LYP/TZ energies. In this latter case, twist-coupled bond shifting would be occurring more readily than conformational automerization. Given the known tendency of B3LYP to overestimate delocalization, this result offers another reason to exercise caution when interpreting B3LYP energies when comparing bond-alternating and bond-equalized annulenes.

Because the BH&HLYP barriers for twist-coupled bond shifting are generally too high, several attempts were made to refine the barrier for **1** → **2** without using intensive cpu-based calculations (i.e., CCSD(T)/cc-pVDZ), but each method used

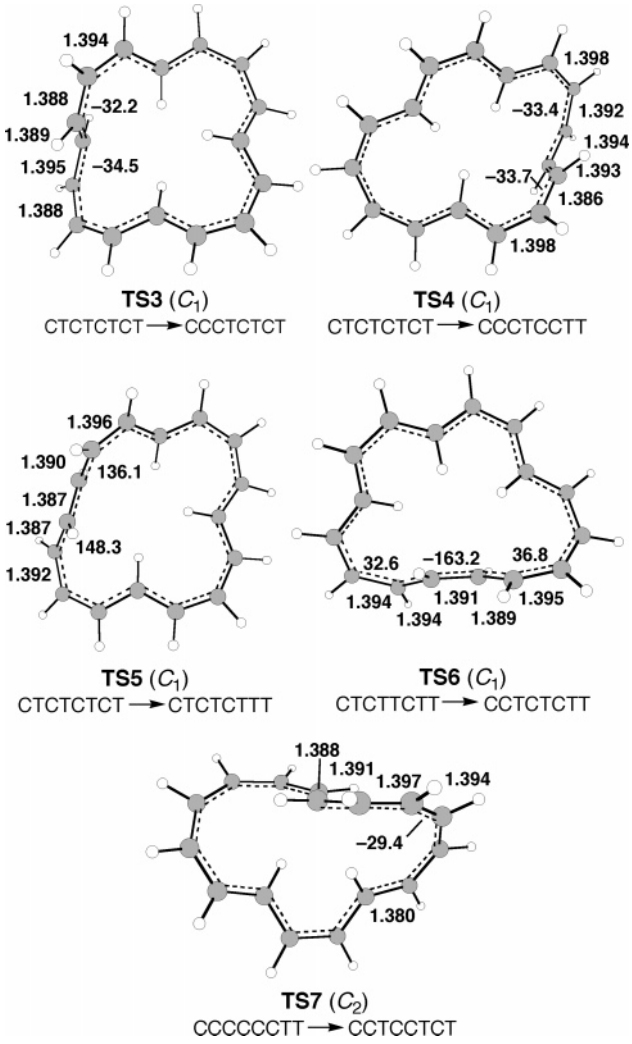

Figure 7. BH&HLYP/6-311+G** structures of additional Möbius bond-shifting transition states in [16]annulene. Selected C−C distances (Å) and CCCC dihedral angles (°) are shown.

also had some attendant ambiguity. The first approach was to determine the single-point energies at the CCSD(T)/6-31G*//BH&HLYP/TZ level. However, prior work of King et al. on [10]annulene using CCSD(T) calculations that omitted polarization functions on hydrogens gave relative energies for the bond-equalized "heart" isomer as compared to the bond-alternating "twist" isomer that were 50% higher than that obtained with their highest level of theory, CCSD(T)/TZ2P//CCSD(T)/DZd.[4b] The single-point energies at the CCSD(T)/6-31G*//BH&HLYP/TZ for [16]annulene **1a** and **TS1**−**2** (Table 1) reveal a ZPE-corrected barrier of 16.1 kcal/mol, an energy that is about 56% too high relative to the experimental one. Our results on configuration change in [12]annulene also show an increased barrier when using CCSD(T)/6-31G.[41] Thus, while the lack of polarization functions on hydrogens gives rise to higher relative energies, it is by no means clear how large the error will be.

An estimate of the CCSD(T) energy with a sufficiently large basis set, i.e., cc-pVDZ, was obtained using the method of McMahon and Bally.[28] We applied this method to numerous relevant stationary points for [16]annulene (Table 1). The only species whose energy is significantly lowered by applying this method is **TS1**−**2**; the barrier for configuration change decreases to 13.7 kcal/mol—much closer to the experimental barrier. This barrier is lowered even further upon using an unrestricted wave function (vide infra).

Table 3. BH&HLYP/6-311+G** Relative Energies (kcal/mol Relative to **1a**) of [16]Annulene Möbius Bond-Shifting Transition States and Adjacent Minima[a]

1c	⇌	**TS1**−**2**	⇌	**2b**
5.3		16.7		5.3
1e	⇌	**TS3**	⇌	CCCTCTCT
6.1		15.6		8.2
1f	⇌	**TS4**	⇌	CCCTCCTT
9.9		21.0		5.0
1a	⇌	**TS5**	⇌	**7**
0.0		21.6		16.7
2a	⇌	**TS6**	⇌	**8**
2.3		20.0		10.5
9	⇌	**TS7**	⇌	**10**
21.4		23.6		19.6

[a] Energies are corrected for differences in ZPE. See Figure 8 for structures of species **1f** and **7**−**10**.

Configuration Change: Other Möbius Transition States and Minima. In addition to locating a transition state for configuration change for **1** → **2**, we located numerous other Möbius bond-shifting transition states, of which five are shown in Figure 7. Three of these—**TS3**, **TS4**, and **TS5**—connect **1** to other configurational isomers. **TS3** arises directly from **1e**, **TS4** arises from a conformation similar to **TS1c1b**, and **TS5** is the bond-equalized version of **TS1a1c**. **TS6** arises from a Möbius conformation of **2**, and **TS7** derives from a hypothetical di-trans isomer studied previously.[8d,10] The DFT barriers and relative energies for the product configurations are shown in Table 3. Based on our CCSD(T)/cc-pVDZ(est) results for **TS1**−**2**, the BH&HLYP energies of **TS3**-**TS7** are likely too high by ca. 3 kcal/mol. At temperatures below those at which electrocyclization occurs, bond shifting via these transition states should be facile. **TS3** represents the lowest energy transition state for configuration change from **1**. This means that if **1** is in equilibrium with **2**, then it is also interconverting with another configuration via **TS3**. However, the adjacent minimum for that configuration (CCCTCTCT) is 8.2 kcal/mol higher than **1a** (BH&HLYP). Detection of that particular species is therefore unlikely.

Of the six bond-shifting transition states reported here, five lead to conformational minima with Möbius topology. Figure 8 depicts the structures of these Möbius minima (**1f** and **7**−**10**), except for **1e** (from **TS3**), which has already been discussed. Like **1e**, species **1f** is another Möbius conformation of **1**, albeit almost 10 kcal/mol above **1a**. Of these Möbius minima, **9** has the smallest Δr value (0.106 Å) and is the only one with clear aromatic character (NICS = −8.3 ppm).[10] Nevertheless, cyclic π overlap presumably is at least partly responsible for these conformations being minima on the PES. Finally, the smaller the torsional angles in the Möbius topology precursor to bond shifting, the lower is the barrier to bond shifting. The interconversion of **9** and **10** via **TS7** is a striking example.

We draw three conclusions from this data: (1) The abundance of Möbius bond-shifting transition states implies that many configurational isomers are likely in solution, but only the dominant ones (e.g., **1a** and **2a**) are detected. (2) Numerous

(41) CCSD(T)/cc-pVDZ single-point energies gave a barrier of 18.0 kcal/mol between the bond alternating tri-*trans* [12]annulene and the Möbius aromatic transition state for bond shifting.[12] Single-point energies using CCSDT)/6-31G* increased this barrier to 19.6 kcal/mol as compared to the experimental barrier (17.4 kcal/mol, Table 2).

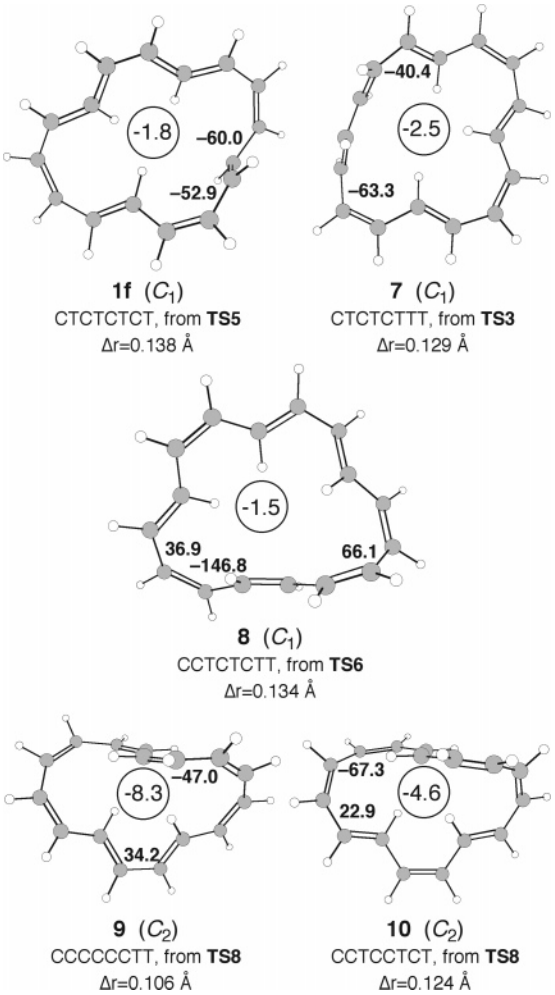

Figure 8. BH&HLYP/6-311+G** structures of Möbius conformational minima of various [16]annulene isomers, obtained by intrinsic reaction coordinate calculations on bond-shifting transition states. CCCC dihedral angles (°) closest to ±90° are shown. B3LYP/TZ GIAO NICS(0) values (ppm) are given in the center of each ring.

Möbius conformational minima (of various configurations) are present in equilibrium with the dominant isomers, albeit in low concentrations. (3) Even if a Möbius [16]annulene were prepared, it would likely isomerize readily to **1a**, due to the many low barriers for configuration change. Efforts to inhibit bond shifting by strategic addition of substituents, or by bridging, would likely perturb the system enough that only a strongly bond-alternating structure would be present.[9]

RHF → UHF Instabilities. According to Heilbronner's early analysis, an ideal bond-equalized Möbius [4*n*]annulene should have a closed-shell electronic structure.[7] Surprisingly, however, the BH&HLYP wave function for **TS1**−**2** has an RHF → UHF instability. The B3LYP wave function, on the other hand, has no such instability. When the BH&HLYP/TZ wave function (not the geometry) is re-optimized using the spin-unrestricted method, the energy drops by 4.4 kcal/mol, resulting in a predicted barrier of 12.3 kcal/mol from **1a**, even closer to the experimental value.[42]

(42) If one then re-optimizes the geometry of **TS1**−**2** using UBH&HLYP and computes the frequencies and zero-point energy with that method as well, the barrier decreases to ca. 10 kcal/mol, virtually identical to the experimentally determined one. This additional lowering arises mainly from the significantly lower ZPE obtained from the spin-unrestricted frequency calculation.

Table 4. DFT RHF → UHF Stability Results for Twist-Coupled Bond-Shifting Transition States in Annulenes[a]

	BH&HLYP		B3LYP
system	stable?	ΔE	stable?
	[16]Annulenes		
TS1−**2**	no	−4.4	yes
TS5	no	−4.6	—[b]
TS3	no	−4.4	yes
TS4	no	−4.2	yes
TS6	no	−5.1	yes
TS7	no	−1.7	yes
	[12]Annulenes		
CTCTCT → CCCTCT	no	−0.6	yes
CTCTCT → CCTCCT	no	−1.1	yes
	[10]Annulene		
CCCCT, two-twist	no	−2.4	yes
	[14]Annulene		
CCCCCCT, two-twist[d]	yes[c]	−	yes[d]

[a] All results were obtained using the 6-311+G** basis set. "stable?" refers to whether the wave function is stable with respect to becoming spin-unrestricted. ΔE = change in absolute energy (kcal/mol) upon re-optimization of the unrestricted wave function (but not the geometry) for unstable cases. [b] No transition state located with B3LYP. [c] Bond-alternating and bond-equalized forms are virtually isoenergetic. Bond-equalized form becomes lower in energy after ZPE correction. [d] Bond-equalized form is a minimum on the PES. See ref 44.

This raises several questions: Is it purely coincidental that the UBH&HLYP barrier is closer to the experimental barrier? Is this method valid for other systems? Do other transition states for twist-coupled bond shifting in annulenes show these instabilities? Re-examination of the key Möbius bond-shifting transition state in [12]annulene[12] also reveals an RHF → UHF instability for the BH&HLYP/TZ wave function (although *not* for B3LYP).[43] While the energies of the transition states are lowered, optimized geometries using an unrestricted wave function are virtually identical to those obtained with restricted wave functions.

Table 4 summarizes RHF → UHF stability results for twisted bond-shifting transition states In [10]-, [12]-, [14]-, and [16]-annulenes. None of these transition states show instabilities when using B3LYP; on the other hand, using BH&HLYP, RHF → UHF instabilities seem to be the rule. The one exception is a degenerate two-twist bond-shifting transition state for CCCCCCT [14]annulene.[44] In this case the worst CCCC torsional angle is only 23.8°. Those with RHF → UHF instabilities have CCCC torsional angles all greater than this value, ranging from 29° to 52°. The energies of all species that show instabilities are decreased when UBH&HLYP is applied.

Inspection of the restricted and unrestricted MOs for **TS1**−**2** (Figure 9) provides a possible explanation for this energy lowering. Restricted MOs 55 and 56, which are nearly degenerate, exhibit numerous bonding and antibonding interactions. In contrast, the pair of spin-unrestricted MOs 55α and 55β are characterized mostly by nonbonding interactions and, more importantly, are largely disjoint (i.e., they have very few atoms

(43) Re-optimizing the [12]annulene bond-shifting transition state and re-computing the frequencies using UBH&HLYP/TZ decreases the relative energy by 3.5 kcal/mol, yielding a barrier that deviates by only 0.7 kcal/mol from the experimental one.

(44) The bond-equalized form of CCCCCCT-[14]annulene (D_2 symmetry) is predicted to be a minimum at the B3LYP/6-31G* and KMLYP/6-31G* levels: Rzepa, H. S. *Org. Lett.* **2005**, *7*, 4637.

(45) (a) Borden, W. T. *J. Am. Chem. Soc.* **1975**, *97*, 5968. (b) Borden, W. T. In *Diradicals*; Borden, W. T., Ed.; Wiley: New York, 1982; pp 1−72.

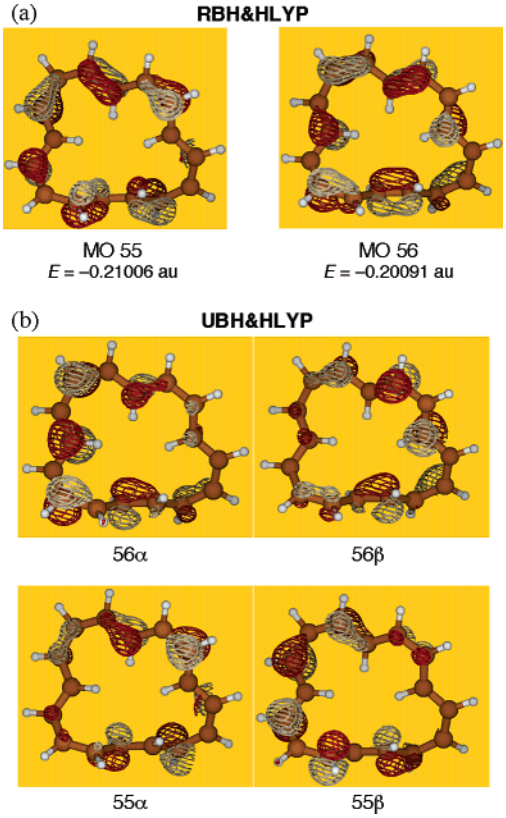

Figure 9. Highest occupied MOs for **TS1**−**2**. (a) RBH&HLYP/6-31G* MOs. Note that 55 and 56 are nearly degenerate. (b) UBH&HLYP/6-31G* spin MOs following re-optimization of the unstable restricted wave function.

in common).[45] The same is true for the pair 56α and 56*β*. Moreover, 55α and 56*β* are largely disjoint with respect to each other, as are 55*β* and 56α. This reduces the electron repulsion between the four electrons in these nearly degenerate MOs,[45] producing a lower energy for the molecule. Presumably the high percentage of Hartree−Fock character in the BH&HLYP functional is the cause of the instabilities in these twisted systems. Indeed, Hartree−Fock calculations on these systems also show such instabilities.

These instabilities are most likely artifacts of the BH&HLYP method. In support of this, T_1 diagnostic values (from coupled cluster calculations) for these bond-shifting transition states are all well below 0.02 (ca. 0.011), indicating that the closed-shell configuration reference wave function is adequate. Nonetheless, the data do indicate that, if an RHF → UHF instability is present, re-optimizing using an unrestricted wave function generally yields a barrier closer to the "true" value.

Conclusions

Using DFT and coupled cluster methods we have located mechanisms for both conformational automerization and configurational isomerization in [16]annulene. Two stepwise pathways are viable for the observed conformational automerization, both of which have computed barriers in excellent agreement with the experimental barrier (ca. 9 kcal/mol). The conformational mobility of [16]annulene is unique in that, unlike [8]- and [12]annulene, it is the first [4*n*]annulene that does not undergo degenerate conformational change via a one-step mechanism.

In addition we present computational evidence that configuration change in [16]annulene proceeds via twist-coupled bond shifting through a Möbius aromatic transition state. The earlier prescient proposal by Oth, that configuration change could proceed via non-isodynamical bond shifts, is correct, except that the bond shifting occurs *not* via planar conformations but rather via highly twisted ones. Our DFT-computed barrier for this process ranges from 16.7 kcal/mol (BH&HLYP/TZ) to 6.9 kcal/mol (B3LYP/TZ). Estimation of a CCSD(T) energy with the cc-pVDZ basis set results in a barrier of 13.7 kcal/mol, in reasonable agreement with the experimental barrier of 10.3 kcal/mol. On the basis of this system and others, B3LYP underestimates bond-shifting barriers, and BH&HLYP overestimates them.

In general, for medium to large annulenes, transition states for conformation change have Möbius topology, and because of this they can serve as starting points for Möbius bond shifting and thus for facile configuration change. Numerous such bond-shifting transition states were located for [16]annulene in this way, and these (1) provide low-energy pathways for interconversion of a variety of configurational isomers and (2) often lead to conformational minima with Möbius topology. The low barriers for twist-coupled bond shifting in [4*n*]annulenes mean that the synthesis of a highly aromatic stable Möbius annulene will be extremely challenging.

Highly nonplanar bond-shifting transition states will show RHF → UHF instabilities when using BH&HLYP, if the CCCC torsional angle is greater than 40°. B3LYP results show no such instabilities. For those annulenes that show these instabilities, re-optimization using an unrestricted wave function appears to provide more reliable barriers.

This work, coupled with our earlier report on [12]annulene,[12] highlights a fundamental contrast with prior accepted work on both [4*n*]- and [4*n* + 2]annulenes. Twist-coupled bond shifting via Möbius topology conformations is distinct from bond shifting via planar conformations in that the latter is known to interconvert degenerate species while the former produces configuration change. Moreover, whereas cis/trans isomerization in acyclic polyenes occurs via a diradical transition state, configuration change in [12]- and [16]annulene occurs via closed-shell, Möbius aromatic transition states. These findings should be general for other annulenes with 4*n* π electrons that can readily attain Möbius topology conformations.

Acknowledgment. We dedicate this paper to Professor J. F. M. Oth. The authors gratefully acknowledge financial support from the Art Furst Scholarship Fund (R.P.P.), the USF Faculty Development Fund, and the National Science Foundation (CHE-0553402).

Supporting Information Available: Tables of absolute energies and zero-point energies, BH&HLYP optimized structures (Cartesian coordinates) of all [16]annulene stationary points, and complete citation for ref 30. This material is available free of charge via the Internet at http://pubs.acs.org.

JA066152X